

## Study the Effect of SiO<sub>2</sub> Nanoparticles as Additive on Corrosion Protection of Steel Rebar in Artificial Concrete Solution

Noor Ali Khudhair and Abdulkareem M.A. Al-Sammarraie  
Department of Chemistry, College of Science, University of Baghdad, Baghdad, Iraq

**Abstract:** It well known the advantages of using SiO<sub>2</sub> nanoparticles as additive for improving the mechanical properties of concrete structure and reducing the liberation of CO<sub>2</sub> gas to the atmosphere. This research investigate the effect of adding SiO<sub>2</sub> nanoparticles (12 nm; 1, 3 and 5% by weight) to artificial concrete solution (2gCa (OH)<sub>2</sub>, 0.0225 g KOH and 0.008 g NaOH in one litter of distilled water) on the corrosion of steel rebar against seawater environment (3.5% NaCl) at four temperatures; 20, 30, 40 and 50°C. The corrosion parameters and pitting probability of the carbon steel rebar were measured in separate experiments using Tafel plot and cyclic polarization procedures, respectively. The corrosion protection efficiency was increased with increasing SiO<sub>2</sub> content and values of 37-80% were recorded in comparison with the concrete solution free of SiO<sub>2</sub>NPs. The cyclic polarization voltagrams show that the SiO<sub>2</sub> NPs reduces the pitting area in all SiO<sub>2</sub> concentrations and fully stopped the pitting problem because of the chloride ions. The surface morphology of the steel rebar was examined before and after polarization using Atomic Force Microscope (AFM).

**Key words:** Corrosion inhibition, nanomaterials, steel rebar, SiO<sub>2</sub>NPs

### INTRODUCTION

The study of the conditions leading to steel rebar corrosion is of high importance because corrosion may significantly affect the load-bearing capacity of reinforced concrete (Wei *et al.*, 2013) and causes widespread damage to critical such as highway bridges sewage pipelines and other critical assets made of concrete (Angst *et al.*, 2009; Ann and Song, 2007). Figure 1 shows the main factors responsible for reinforcement corrosion, carbonation induces a generalized corrosion while the presence of chloride ions in the surroundings of the steel leads to localized corrosion (Figueira *et al.*, 2017).

The main sources of chlorides for concrete structures are marine environments and the use of deicing salts in

roads in cold climates (Alonso *et al.*, 2000). While carbonation implies a gas that needs the pore network partially empty (Pacheco, 2015).

Many strategies were used to decreases the risk of concrete corrosion (Paul and Van Zijl, 2017; Zhao *et al.*, 2017) such as using additives to the concrete mix (Goyal *et al.*, 2018; Bamforth, 2004), coating the steel rebar and others (Bamforth, 2004; Broomfield, 2006; Berrocal *et al.*, 2016; Osial and Wilinski, 2016).

Nanomaterials has become one of the best choice for enhancing corrosion resistance, several materials have been used for this goal such as ceramic materials and others (Raki *et al.*, 2010; Lin *et al.*, 2008; Sato and Beaudoin, 2007; Anaee, 2015; Shen *et al.*, 2005; Xiong *et al.*, 2006).

The present work designed to study the influence adding SiO<sub>2</sub> NPs on the corrosion rates and of pitting probability of the steel rebar imbedded in concrete containing 3.5% NaCl.

### MATERIALS AND METHODS

The steel rebar which used in this study was (Ukraine origin) with diameter of 16 mm and its chemical composition is given by the manufacturer and listed in Table 1.

Prior to do the polarization experiments the steel rebar was deoxidized by immersion in concentrated HCl (37%, Fluka/Switzerland), followed by rinsing with running tap water and then dewatered with ethanol and

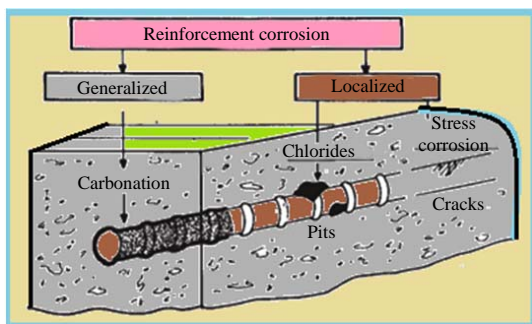


Fig. 1: Scheme represents factors responsible for corrosion of steel bar in concrete

left to dry, the steel sample serve as working electrode was warped with adhesive tape except for a known distance which was (16.55 cm<sup>2</sup>), Pt-electrode serve as counter electrode and Ag/AgCl as references electrode.

Then, the steel rebar polarized in the concrete simulation solution (Ca (OH)<sub>2</sub> (2 g), KOH (0.02244 g), NaOH (0.008 g) in 1L of distilled containing 3.5% NaCl and SiO<sub>2</sub> NPs (12 nm, Degussa, Germany) in different concentration (1, 3 and 5%) as additive. After that, Tafel plots were recorded for corrosion rate measurement by scanning the potentials ±200 mV around the OCP with a rate of 2 mV sec<sup>-1</sup>. The same procedure repeated at four temperatures 20, 30, 40 and 50°C.

Table 1: Chemical composition of the steel rebar used in this study

Elements	Percentage
C	0.260
S	0.031
Si	0.280
N	0.010
Cu	0.280
Mn	0.730
Ni	0.130
Cr	0.120

For pitting corrosion investigation the steel rebar subjected to a cyclic polarization at 20°C starting from few millivolt lower than OCP going up to about 1000 mV. Atomic force microscope (SPM AA3000, Angstrom Advanced Inc., USA) was used to study the change in the morphology of the steel rebar surface before and after polarization.

**RESULTS AND DISCUSSION**

Figure 2 show the recorded Tafel plots for the steel rebar in simulated concrete solution containing 3.5% NaCl, without and with adding SiO<sub>2</sub> NPs (1, 3 and 5%), at temperatures of 20, 30, 40 and 50°C.

All corrosion parameters including E<sub>corr</sub> in (millivolt), I<sub>corr</sub> in (ampere), weight loss in (g.m<sup>-2</sup>.d<sup>-1</sup>), penetration loss in (mmper year (mmpy)) were measured and calculated from above Tafel plots while polarization resistance Rp in (Ω.cm<sup>2</sup>) and corrosion protection efficiency (%) were calculated using the Eq. 1 and 2 (Kaesche, 2003) are listed in Table 1:

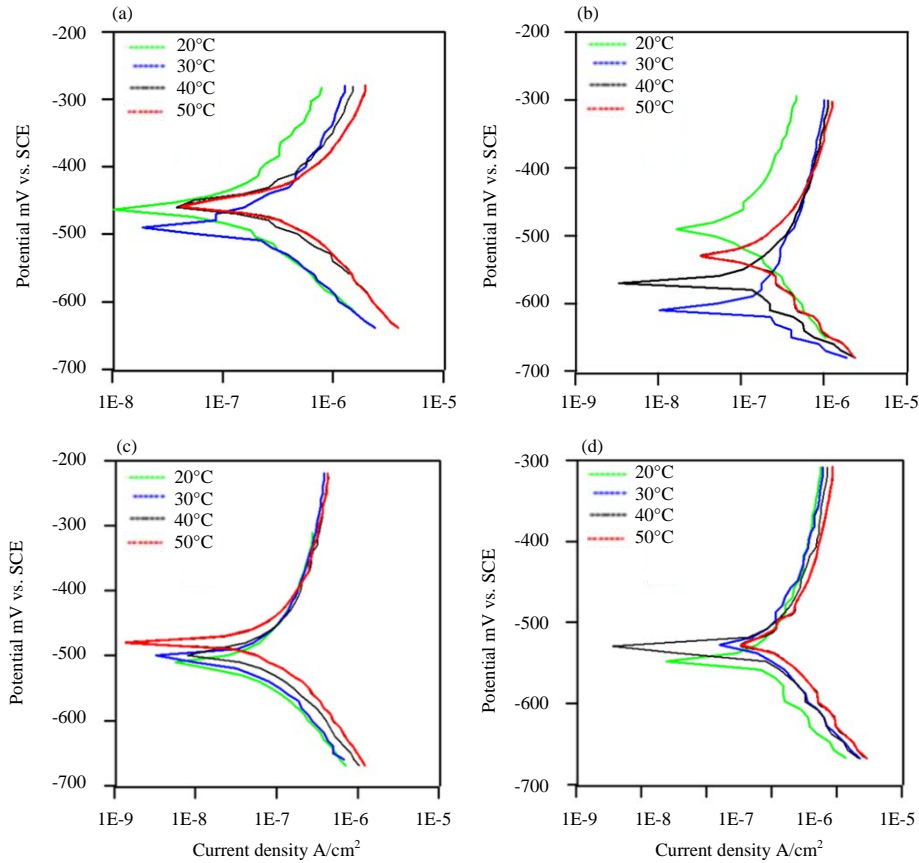


Fig. 2(a-d): Tafel plots of steel rebar polarized in simulated concrete solution containing TiO<sub>2</sub> NPs (a) Without, (b) -1, (c) -3.0 and (d) -5.0%) with 3.5% NaCl and different temperatures

Table 2: Corrosion rate parameters of steel rebar polarized in simulated concrete solution containing SiO<sub>2</sub> NPs (12 nm) and 3.5% NaCl at 20, 30, 40, 50°C

SiO <sub>2</sub> (%)	T (K)	E <sub>corr</sub> (mV)	i <sub>corr</sub> (A*10 <sup>-6</sup> cm <sup>-2</sup> )	β <sub>c</sub> (mV/Dec)	β <sub>a</sub> (mV/Dec)	R <sub>p</sub> Ω.cm <sup>2</sup>	CR (WL) g.m <sup>-2</sup> .d <sup>-1</sup>	CR (PL) mmpy	PE (%)
0	293	-458.7	95.86	-125.1	145.5	2799.85	24.00	1.110	-
	303	-478.1	100.76	-91.6	102.1	2112.44	25.20	1.170	-
	313	-467.8	215.79	97.6	176.3	5886.36	53.90	2.500	-
	323	-457.1	257.57	-123.6	142.3	7397.86	64.40	2.990	-
1	293	-431.2	56.24	-143.7	145.6	1766.12	14.10	0.653	41.33
	303	-468.3	77.07	-118.4	137.3	2127.56	19.30	08.950	23.51
	313	-458.8	81.29	-104.6	120.9	1979.49	20.30	0.944	62.32
	323	-448.4	90.52	-106.2	132.6	2317.84	22.60	1.050	64.85
3	293	-509.7	46.45	-122.8	169.3	1435.54	11.60	0.539	51.54
	303	-503.9	62.94	-149.0	224.7	2448.49	15.70	0.731	37.53
	313	-477.7	68.29	-134.3	194.2	2354.25	17.10	0.793	68.35
	323	-477.6	77.11	-148.4	217.8	2955.22	19.30	0.895	70.06
5	293	-524.9	27.39	-124.4	183.5	881.74	6.85	0.318	71.42
	303	-509.0	35.12	-131.8	181.9	1165.45	8.78	0.408	65.14
	313	-491.6	41.95	-136.7	192.4	1455.74	10.50	0.487	80.55
6	323	-475.4	46.46	-145.4	216.7	1755.41	11.60	0.539	81.96

$$R_p = \frac{\beta_a \beta_c}{2.303(i_{corr})(\beta_a + \beta_c)} \quad (1)$$

Where, β<sub>a</sub> and β<sub>c</sub> are Tafel slopes:

$$IE\% = \frac{i_{corr}(wo)^{-1} \text{Corr}(W)}{i_{corr}(Wo)} \times 100 \quad (2)$$

Where, i<sub>corr</sub> (wo) and i<sub>corr</sub> (w) are the corrosion current without and with using SiO<sub>2</sub>NPs, respectively (Table 2).

The R<sub>p</sub> values were decreased with adding SiO<sub>2</sub> NPs which may attributed to the metallic property of the steel rebar which remain unaffected by corrosion in comparison with SiO<sub>2</sub> free concrete as the corrosion product (Iron oxides) have less electrical conductivity (Hashim and Kassim, 2014).

The corrosion Protection Efficiency(PE%) increased with increasing the added amount of SiO<sub>2</sub> NPs, this result may explained by the effect of SiO<sub>2</sub> to stabilized the protective layer on the steel rebar (Razaqpur and Isgor, 2009). A maximum PE was achieved on using 5% SiO<sub>2</sub> while using 1% SiO<sub>2</sub> exhibited the lowest PE (23%). The thermodynamic properties (E<sub>a</sub>, G\*, H\* and S\*) were calculated using the following relationships (Abeng *et al.*, 2017):

$$\text{Log CR} = \text{log A} - \frac{E_a}{2.303RT} \quad (3)$$

$$\text{Log} \frac{CR}{T} = \text{log} \left( \frac{R}{Nh} \right) + \frac{\Delta S_a}{2.303R} - \frac{\Delta H_a}{2.303RT} \quad (4)$$

Where:

- R : The universal gas constant (8.314 J mol<sup>-1</sup> K<sup>-1</sup>)
- T : The temperature (K)
- h : The Plank's constant (6.626176×10<sup>-34</sup> Js)
- N : The Avogadro's number (6.022×10<sup>23</sup> mol<sup>-1</sup>)
- ΔS<sub>a</sub> : The entropy of activation
- ΔH<sub>a</sub> : The enthalpy of activation

Table 3: Thermodynamic function (E<sub>a</sub>, ΔH\*, ΔS\* and ΔG\*) of steel rebar in/concrete electrolyte solution containing 3.5 NaCl and SiO<sub>2</sub> NPs

SiO <sub>2</sub> (%)	T (K)	E <sub>a</sub> (kJ/mole)	ΔH* (kJ/mol)	ΔS* (kJ/mol.K)	ΔG* (kJ/mol)
0	293	16.090	18.569	-0.144	60.761
	303				62.201
	313				63.641
	323				65.081
1	293	12.485	6.467	-0.188	61.551
	303				63.431
	313				65.311
	323				67.191
3	293	13.296	7.218	-0.187	62.009
	303				63.879
	313				65.749
	323				67.619
5	293	13.861	8.371	-0.188	63.455
	303				65.335
	313				67.217
	323				69.095

Then, G can calculated using Eq. 4:

$$\Delta G_a = \Delta H_a - T\Delta S_a \quad (5)$$

All thermodynamic functions are tabulated in Table 3. The values of energy of activation (E<sub>a</sub>) do not indicates a reduction of the corrosion rates with adding SiO<sub>2</sub> content buit changing the properties the steel surface lead to decreasing the corrosion rate in the concrete solution (Novoa, 2016).

The enthalpy of activation of the corrosion process (ΔH\*) took positive value which reflected endothermic process and also decreased with increasing SiO<sub>2</sub> contents (Fig. 3 and 4).

Values of the calculated ΔG\* were nearly constant and have positive value at all temperature which describe the process as non-spontaneous. The negative values of the entropy means that the reactant had some degree of

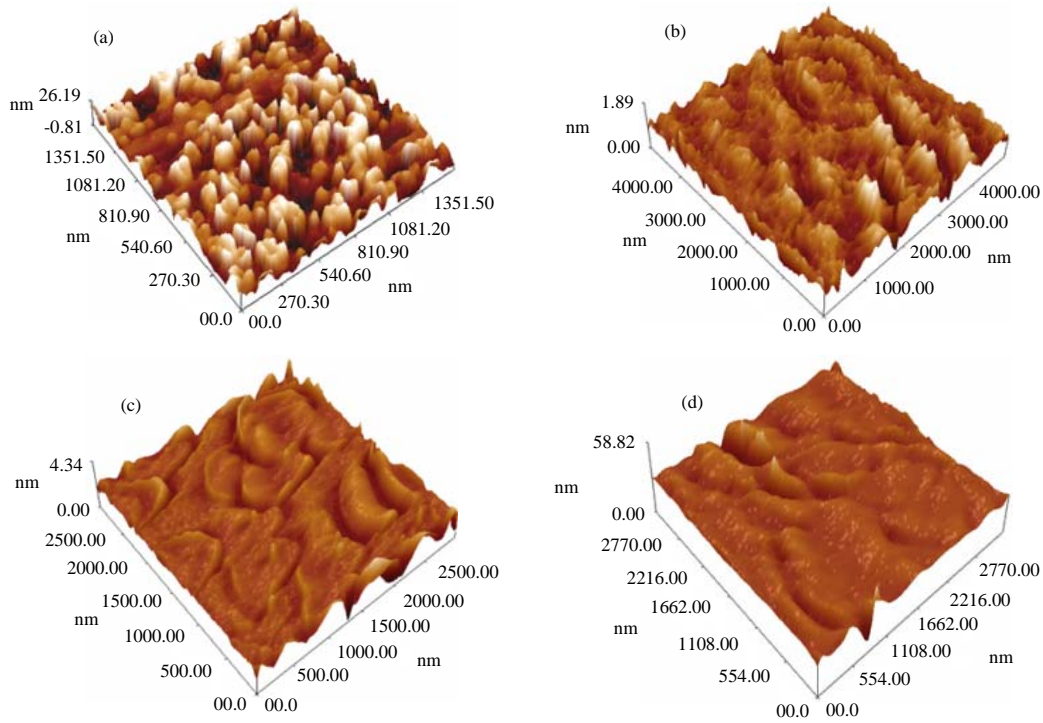


Fig. 3(a-d): AFM 3D views of steel rebar polarized in artificial concrete solution containing 3.5% NaCl, (a) Without  $\text{SiO}_2$  NPs and with adding  $\text{SiO}_2$  NPs (12 nm) (b) -1, (c) -3 and (d) -5%

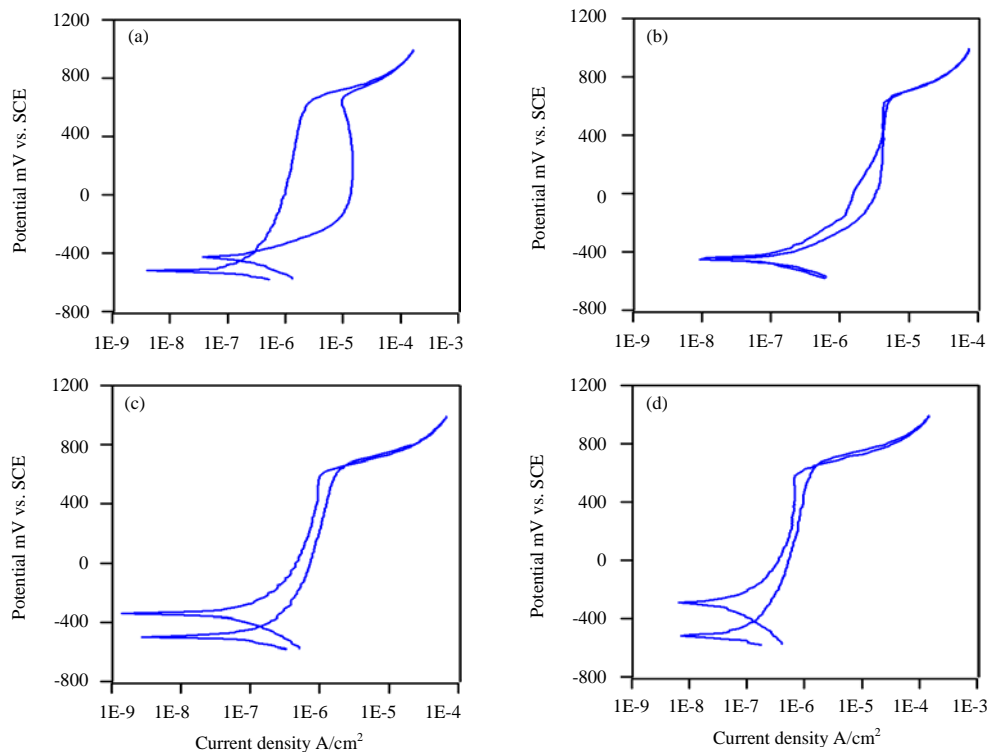


Fig. 4(a-d): Cyclic polarization voltammogram of steel rebar polarized in artificial concrete solution containing 3.5% NaCl, (a) Without  $\text{SiO}_2$  NPs and with adding  $\text{SiO}_2$  NPs (12 nm) (b) -1%, (c) -3% and (d) -5% at 20°C

freedom and it reduced by increasing the SiO<sub>2</sub> content and remain constant at all concentrations. The surface morphology changing was examined by Atomic force microscope as shown in (Fig. 3).

These images clearly supported the investigations deduced from the electrochemical polarization procedure, since, the surface morphology in 3.5% NaCl without using SiO<sub>2</sub> is very rough containing deep valley (Fig. 3a) while the surface roughness on using SiO<sub>2</sub> NPs reduced SiO<sub>2</sub> Fig. 3b-d.

The probability of pitting corrosion occurrences was investigated by cyclic polarization procedure (Ebell *et al.*, 2016; Chauhan and Sharma, 2019; Gu *et al.*, 2018) as mentioned in the experimental part, Fig. 3 shows the cyclic Volta grams and the histories loops which have formed during the polarization in each solution. A pitting at high positive pitting potentials with very small histories loop area for the steel rebar in simulate concrete electrolyte with different concentrations of SiO<sub>2</sub> as additive and 3.5% NaCl (Fig. 4a-d).

These polarizations voltagram show that remarkable pitting area produced when cyclic polarization conducted for steel rebar in simulate concrete solution with 3.5% NaCl without adding SiO<sub>2</sub> NPs. In another hand the SiO<sub>2</sub> NPs at all concentrations reduces the pitting area and fully diminished the pitting problem.

## CONCLUSION

The following conclusions have drawn from this research; all SiO<sub>2</sub> concentration lead to enhancing the corrosion protection efficiency of steel rebar in concrete at seawater environment. The pitting corrosion of the steel rebar is totally overcome on using SiO<sub>2</sub> NPs.

## REFERENCES

- Abeng, F.E., V.D. Idim and P.J. Nna, 2017. Kinetics and thermodynamic studies of corrosion inhibition of mild steel using methanolic extract of erigeron floribundus (Kunth) in 2 M HCl solution. *World News Nat. Sci.*, 10: 26-38.
- Alonso, C., C. Andrade, M. Castellote and P. Castro, 2000. Chloride threshold values to depassivate reinforcing bars embedded in a standardized OPC mortar. *Cem. Concr. Res.*, 30: 1047-1055.
- Anae, R.A., 2015. Corrosion protection of steel using nano ceramic particles coating. M.Sc. Thesis, University of Technology Iraq, Baghdad, Iraq.
- Angst, U., B. Elsener, C.K. Larsen and O. Vennesland, 2009. Critical chloride content in reinforced concrete-A review. *Cem. Concr. Res.*, 39: 1122-1138.
- Ann, K.Y. and H.W. Song, 2007. Chloride threshold level for corrosion of steel in concrete. *Corrosion Sci.*, 49: 4113-4133.
- Bamforth, P.B., 2004. Enhancing Reinforced Concrete Durability: Guidance on Selecting Measures for Minimising the Risk of Corrosion of Reinforcement in Concrete. The Concrete Society, London, UK., ISBN: 9781904482116, Pages: 208.
- Berrocal, C.G., K. Lundgren and I. Lofgren, 2016. Corrosion of steel bars embedded in fibre reinforced concrete under chloride attack: State of the art. *Cem. Concr. Res.*, 80: 69-85.
- Broomfield, J.P., 2006. Corrosion of Steel in Concrete: Understanding, Investigation and Repair. 2nd Edn., CRC Press, Boca Raton, Florida, USA., ISBN: 9780415334044, Pages: 296.
- Chauhan, A. and U.K. Sharma, 2019. Influence of temperature and relative humidity variations on non-uniform corrosion of reinforced concrete. *Structures*, 19: 296-308.
- Ebell, G., A. Burkert, J. Fischer, J. Lehmann, T. Muller, D. Meinel and O. Paetsch, 2016. Investigation of chloride induced pitting corrosion of steel in concrete with innovative methods. *Mater. Corros.*, 67: 583-590.
- Figueira, R.B., A. Sadowski, A.P. Melo and E.V. Pereira, 2017. Chloride threshold value to initiate reinforcement corrosion in simulated concrete pore solutions: The influence of surface finishing and pH. *Constr. Build. Mater.*, 141: 183-200.
- Goyal, A., H.S. Pouya, E. Ganjian and P. Claisse, 2018. A review of corrosion and protection of steel in concrete. *Arabian J. Sci. Eng.*, 43: 5035-5055.
- Gu, X., H. Guo, B. Zhou, W. Zhang and C. Jiang, 2018. Corrosion non-uniformity of steel bars and reliability of corroded RC beams. *Eng. Struct.*, 167: 188-202.
- Hashim, N.Z.N. and K. Kassim, 2014. The effect of temperature on mild steel corrosion in 1 M HCl by schiff bases. *Malaysian J. Anal. Sci.*, 18: 28-36.
- Kaesche, H., 2003. Chemical Thermodynamics of Corrosion. In: *Corrosion of Metals*, Kaesche, H. (Ed.). Springer, Berlin, Germany, ISBN: 978-3-642-05620-8, pp: 11-55.
- Lin, K.L., W.C. Chang, D.F. Lin, H.L. Luo and M.C. Tsai, 2008. Effects of nano-SiO<sub>2</sub> and different ash particle sizes on sludge ash-cement mortar. *J. Environ. Manage.*, 88: 708-714.
- Novoa, X.R., 2016. Electrochemical aspects of the steel concrete system: A review. *J. Solid State Electrochem.*, 20: 2113-2125.
- Osial, M. and D. Wilinski, 2016. Organic substances as corrosion inhibitors for steel in concrete-An overview. *J. Build. Chem.*, 1: 43-53.
- Pacheco F.J., 2015. Corrosion of steel in cracked concrete: Chloride microanalysis and service life predictions. Ph.D. Thesis, Delft University of Technology (TU Delft), Delft, Netherlands.
- Paul, S.C. and G.P.A.G. Van Zijl, 2017. Corrosion deterioration of steel in cracked SHCC. *Int. J. Concr. Struct. Mater.*, 11: 557-572.

- Raki, L., J. Beaudoin, R. Alizadeh, J. Makar and T. Sato, 2010. Cement and concrete nanoscience and nanotechnology. *Materials*, 3: 918-942.
- Razaqpur, A. and O. Isgor, 2009. Prediction of Reinforcement Corrosion in Concrete Structures. In: *Frontier Technologies for Infrastructure Engineering*, Ang, A.H. and S.S. Chen (Eds.). CRC Press, Boca Raton, Florida, USA., pp: 45-68.
- Sato, T. and J.J. Beaudoin, 2007. The Effect of nano-sized  $\text{CaCO}_3$  addition on the hydration of cement paste containing high volumes of fly ash. *Proceedings of the 12th International Congress on the Chemistry of Cement*, July 8-13, 2007, National Research Council Canada, Montreal, Quebec, Canada, pp: 1-12.
- Shen, G.X., Y.C. Chen, L. Lin, C.J. Lin and D. Scantlebury, 2005. Study on a hydrophobic nano- $\text{TiO}_2$  coating and its properties for corrosion protection of metals. *Electrochim. Acta*, 50: 5083-5089.
- Wei, J., J.H. Dong and W. Ke, 2013. Corrosion evolution of scaled rebar in concrete under dry/wet cyclic condition in 3.5% NaCl solution. *Int. J. Electrochem. Sci.*, 8: 2536-2550.
- Xiong, G., M. Deng, L. Xu and M. Tang, 2006. Properties of cement-based composites by doping nano- $\text{TiO}_2$ . *J. Chin. Ceram. Soc.*, 34: 1158-1161.
- Zhao, X., C. Chen, W. Xu, Q. Zhu, C. Ge and B. Hou, 2017. Evaluation of long-term corrosion durability and self-healing ability of scratched coating systems on carbon steel in a marine environment. *Chin. J. Oceanol. Limnol.*, 35: 1094-1107.